
Statistically Valid Variable Importance Assessment through Conditional Permutations (Supplementary Material)

Anonymous Author(s)

Affiliation

Address

email

1 A Conditional Permutation Importance (CPI) Wald statistic asymptotically 2 controls type-I errors: hypotheses, theorem and proof

3 **Outline** The proof relies on the observation that the importance score defined in (4) is 0 in the
4 asymptotic regime, where the permutation procedure becomes a sampling step, under the assumption
5 that variable j is not conditionally associated with y . Then all the proof focuses on the convergence of
6 the finite-sample estimator to the population one. To study this, we use the framework developed in
7 [Williamson et al., 2021]. Note that the major difference with respect to other contributions [Watson
8 and Wright, 2021] is that the ensuing inference is no longer conditioned on the estimated learner $\hat{\mu}$.
9 Next, we first restate the precise technical conditions under which the different importance scores
10 considered are asymptotically valid, i.e. lead to a Wald-type statistic that behaves as a standard
11 normal under the null hypothesis.

12 **Notations** Let \mathcal{F} represent the class of functions from which a learner $\mu : \mathbf{x} \mapsto y$ is sought.

13 Let P_0 be the data-generating distribution and P_n is the empirical data distribution observed after
14 drawing n samples (noted n_{train} in the main text; in this section, we denote it n to simplify
15 notations). The separation between train and test samples is actually only relevant to alleviate
16 some technical conditions on the class of learners used. \mathcal{M} is the general class of distributions
17 from which P_1, \dots, P_n, P_0 are drawn. $\mathcal{R} := \{c(P_1 - P_2) : c \in [0, \infty), P_1, P_2 \in \mathcal{M}\}$ is the
18 space of finite signed measures generated by \mathcal{M} . Let l be the loss function used to obtain μ .
19 Given $f \in \mathcal{F}$, $l(f; P_0) = \int l(f(\mathbf{x}), y) P_0(\mathbf{z}) d\mathbf{z}$, where $\mathbf{z} = (\mathbf{x}, y)$. Let μ_0 denote a population
20 solution to the estimation problem $\mu_0 \in \operatorname{argmin}_{f \in \mathcal{F}} l(f; P_0)$ and $\hat{\mu}_n$ a finite sample estimate $\hat{\mu}_n \in$
21 $\operatorname{argmin}_{f \in \mathcal{F}} l(f; P_n) = \frac{1}{n} \sum_{(\mathbf{x}, y) \in P_n} l(f(\mathbf{x}), y)$.

22 Let us denote by $\dot{l}(\mu, P_0; h)$ the Gâteaux derivative of $P \mapsto l(\mu, P)$ at P_0 in the direction $h \in \mathcal{R}$,
23 and define the random function $g_n : \mathbf{z} \mapsto \dot{l}(\hat{\mu}_n, P_0; \delta_{\mathbf{z}} - P_0) - \dot{l}(\mu_0, P_0; \delta_{\mathbf{z}} - P_0)$, where $\delta_{\mathbf{z}}$ is the
24 degenerate distribution on $\mathbf{z} = (\mathbf{x}, y)$.

25 Hypotheses

26 (A1) (Optimality) there exists some constant $C > 0$, such that for each sequence $\mu_1, \mu_2, \dots \in \mathcal{F}$
27 given that $\|\mu_n - \mu_0\| \rightarrow 0$, $|l(\mu_n, P_0) - l(\mu_0, P_0)| < C \|\mu_n - \mu_0\|_{\mathcal{F}}^2$ for each n large
28 enough.

29 (A2) (Differentiability) there exists some constant $\kappa > 0$ such that for each sequence $\epsilon_1, \epsilon_2, \dots \in$
30 \mathbb{R} and $h_1, h_2, \dots \in \mathcal{R}$ satisfying $\epsilon_n \rightarrow 0$ and $\|h_n - h_\infty\| \rightarrow 0$, it holds that

$$\sup_{\mu \in \mathcal{F}: \|\mu - \mu_0\|_{\mathcal{F}} < \kappa} \left| \frac{l(\mu, P_0 + \epsilon_n h_n) - l(\mu, P_0)}{\epsilon_n} - \dot{l}(\mu, P_0; h_n) \right| \rightarrow 0.$$

- 31 (A3) (Continuity of optimization) $\|\mu_{P_0+\epsilon h} - \mu_0\|_{\mathcal{F}} = O(\epsilon)$ for each $h \in \mathcal{R}$.
32 (A4) (Continuity of derivative) $\mu \mapsto \dot{l}(\mu, P_0; h)$ is continuous at μ_0 relative to $\|\cdot\|_{\mathcal{F}}$ for each
33 $h \in \mathcal{R}$.
34 (B1) (Minimum rate of convergence) $\|\hat{\mu}_n - \mu_0\|_{\mathcal{F}} = o_P(n^{-1/4})$.
35 (B2) (Weak consistency) $\int g_n(\mathbf{z})^2 dP_0(\mathbf{z}) = o_P(1)$.
36 (B3) (Limited complexity) there exists some P_0 -Donsker class \mathcal{G}_0 such that $P_0(g_n \in \mathcal{G}_0) \rightarrow 1$.

37 **Proposition** (Theorem 1 in [Williamson et al., 2021]) If the above conditions hold, $l(\hat{\mu}_n, P_n)$ is an
38 asymptotically linear estimator of $l(\mu_0, P_0)$ and $l(\hat{\mu}_n, P_n)$ is non-parametric efficient.

39 Let P_0^* be the distribution obtained by sampling the j -th coordinate of \mathbf{x} from the conditional
40 distribution of $q_0(x^j|\mathbf{x}^{-j})$, obtained after marginalizing over y :

$$q_0(x^j|\mathbf{x}^{-j}) = \frac{\int P_0(\mathbf{x}, y) dy}{\int P_0(\mathbf{x}, y) dx^j dy}$$

41 $P_0^*(\mathbf{x}, y) = q_0(x^j|\mathbf{x}^{-j}) \int P_0(\mathbf{x}, y) dx^j$. Similarly, let P_n^* denote its finite-sample counterpart. It
42 turns out from the definition of \hat{m}_{CPI}^j in Eq. 4 that $\hat{m}_{CPI}^j = l(\hat{\mu}_n, P_n^*) - l(\hat{\mu}_n, P_n)$. It is thus the
43 final-sample estimator of the population quantity $m_{CPI}^j = l(\hat{\mu}_0, P_0^*) - l(\hat{\mu}_0, P_0)$.

44 Given that $\hat{m}_{CPI}^j = l(\hat{\mu}_n, P_n^*) - l(\hat{\mu}_0, P_0^*) - (l(\hat{\mu}_n, P_n) - l(\hat{\mu}_0, P_0)) + l(\hat{\mu}_0, P_0^*) - l(\hat{\mu}_0, P_0)$, the
45 estimator \hat{m}_{CPI}^j is asymptotically linear and non-parametric efficient.

46 The crucial observation is that under the j -null hypothesis, y is independent of x^j given \mathbf{x}^{-j} . Indeed,
47 in that case $P_0(\mathbf{x}, y) = q_0(x^j|\mathbf{x}^{-j})P_0(y|\mathbf{x}^{-j})P_0(\mathbf{x}^{-j})$ and $P_0(x^j|\mathbf{x}^{-j}, y) = P_0(x^j|\mathbf{x}^{-j})$, so that
48 $P_0^* = P_0$. Hence, mean/variance of \hat{m}_{CPI}^j 's distribution provide valid confidence intervals for m_{CPI}^j
49 and $mean(\hat{m}_{CPI}^j) \xrightarrow{n \rightarrow \infty} 0$. Thus, the Wald statistic \hat{z}_{CPI}^j defined in section (4.2) converges to a
50 standard normal distribution, implying that the ensuing test is valid.

51 In practice, hypothesis (B3), which is likely violated, is avoided by the use of cross-fitting as discussed
52 in [Williamson et al., 2021]: as stated in the main text, variable importance is evaluated on a set of
53 samples not used for training. An interesting impact of the cross-fitting approach is that it reduces the
54 hypotheses to (A1) and (A2), plus the following two:

- 55 (B'1) (Minimum rate of convergence) $\|\hat{\mu}_n - \mu_0\|_{\mathcal{F}} = o_P(n^{-1/4})$ on each fold of the sample
56 splitting scheme.
57 (B2') (Weak consistency) $\int g_n(\mathbf{z})^2 dP_0(\mathbf{z}) = o_P(1)$ on each fold of the sample splitting scheme.

58 B Evaluation Metrics

59 **AUC score** [Bradley, 1997]: The variables are ordered by increasing p-values, yielding a family of
60 p splits into relevant and non-relevant at various thresholds. AUC score measures the consistency of
61 this ranking with the ground truth ($n_{signals}$ predictive features versus $p - n_{signals}$).

62 **Type-I error** : Some methods output p-values for each of the variables, that measure the evidence
63 against each variable being a null variable. This score checks whether the rate of low p-values of null
64 variables is not exceeding the nominal false positive rate (set to 0.05).

65 **Power** : This score reports the average proportion of informative variables detected (when consid-
66 ering variables with p-value < 0.05).

67 **Computation time** : The average computation time per core on 100 cores.

68 **Prediction Scores** : As some methods share the same core to perform inference and with the data
69 divided into a train/test scheme, we evaluate the predictive power for the different cores on the test
70 set.

71 **C Supplement Figure 1 - Diagram of CPI**

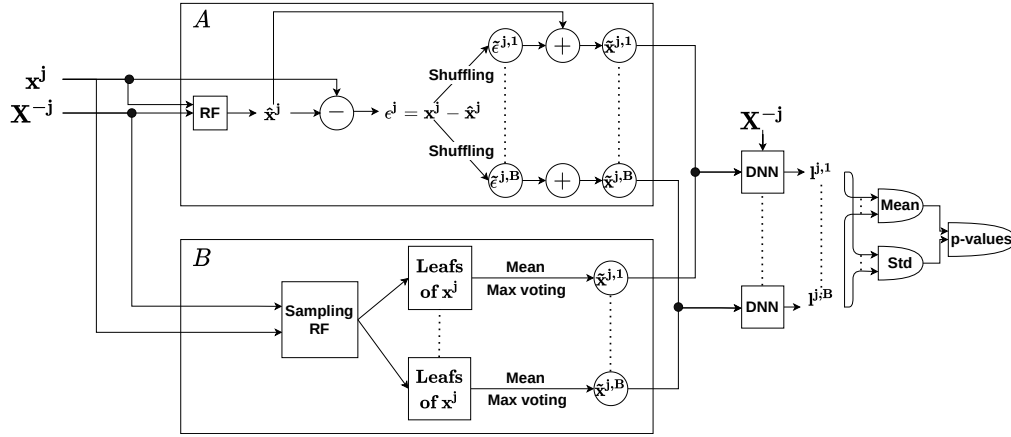


Figure 1: **CPI-DNN’s constructions:** Constructing the variable of interest \bar{x}^j is done either (1) by the additive construction (top block) where a shuffled version of the residuals is added to the predicted version using the remaining predictors with the mean of a random forest (RF) or (2) by the sampling construction (bottom block) using a random forest (RF) model to fit x^j from X^{-j} and then sample the prediction within the leaves of the RF.

72 **D Supplement Figure 1 - Power & Computation time**

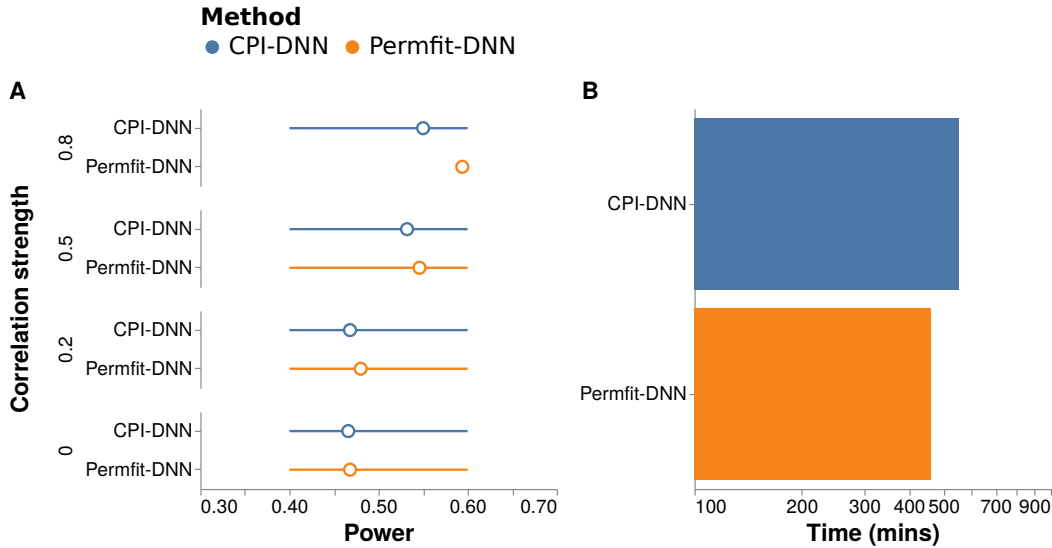


Figure 2: **Permfit-DNN vs CPI-DNN:** Performance at detecting important variables on simulated data under the setting of experiment 1, with $n = 300$ and $p = 100$. (A): The power reports the average proportion of informative variables detected ($p\text{-value} < 0.05$). (B): The computation time is in mins with (log10 scale) per core on 100 cores.

73 Based on Fig. 2, both methods *Permfit-DNN* and *CPI-DNN* have almost similar power. In high
 74 correlation regime, *Permfit-DNN* yields more detections, but it does not control type-I errors (Fig. 1).
 75 Regarding computation time, *CPI-DNN* is slightly more computationally expensive than *Permfit-DNN*.
 76

77 **E Supplement Figure 3 - Extended model comparisons**

78 We also benchmarked the following methods deprived of statistical guarantees:

- 79 • Knockoffs [Candes et al., 2017, Nguyen et al., 2020]: The knockoff filter is a variable selection method for multivariate models that controls the False Discovery Rate. The first step of this procedure involves sampling extra null variables that have a correlation structure similar to that of the original variables. A statistic is then calculated to measure the strength of the original variables versus their knockoff counterpart. We call this the knockoff statistic $\mathbf{w} = \{w_j\}_{j=1}^p$, that is the difference between the importance of a given feature and the importance of its knockoff.
- 86 • Approximate Shapley values [Burzykowski, 2020]: SHAP being an instance method, we relied on an aggregation (averaging) of the per-sample Shapley values.
- 88 • Shapley Additive Global importanceE (SAGE) [Covert et al., 2020]: Whereas SHAP focuses on the *local interpretation* by aiming to explain a model’s individual predictions, SAGE is an extension to SHAP assessing the role of each feature in a *global interpretability* manner. The SAGE values are derived by applying the Shapley value to a function that represents the predictive power contained in subsets of features.
- 93 • Mean Decrease of Impurity [Louppe et al., 2013]: The importance scores are related to the impact that each feature has on the impurity function in each of the nodes.
- 95 • BART [Chipman et al., 2010]: BART is an ensemble of additive regression trees. The trees are built iteratively using a back-fitting algorithm such as MCMC (Markov Chain Monte Carlo). By keeping track of covariate inclusion frequencies, BART can identify which components are more important for explaining y .

99 Based on AUC, we observe SHAP, SAGE and Mean Decrease of Impurity (MDI) perform poorly. These approaches are vulnerable to correlation. Next, Knockoff-Deep and Knockoff-Lasso perform well when the model does not include interaction effects. BART and Knockoff-Bart show fair performance overall.

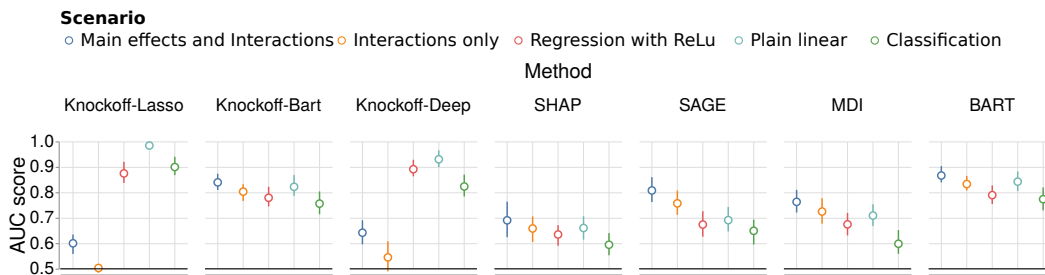


Figure 3: **Extended model comparisons:** State-of-the-art methods for variable importance not providing statistical guarantees in terms of p-values are compared (outer columns) and to competing approaches across data-generating scenarios (inner columns) using the settings of experiments 2 and 3. Prediction tasks were simulated with $n = 1000$ and $p = 50$. Solid line: chance level.

102

103 **F Supplement Figure 3 - Power**

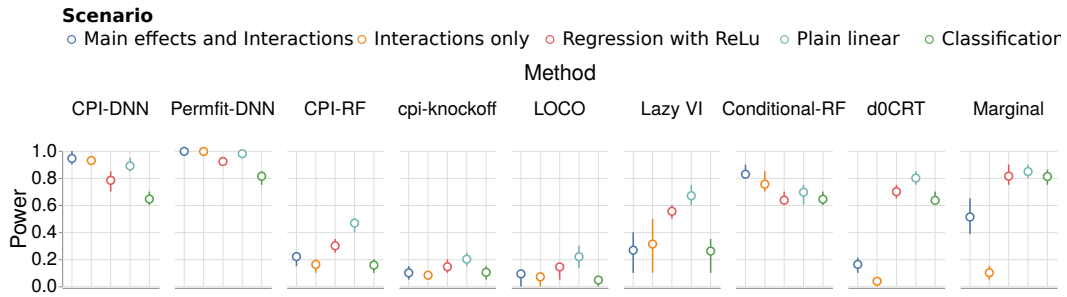


Figure 4: **Extended model comparisons:** *CPI-DNN* and *Permfit-DNN* were compared to baseline models (outer columns) and to competing approaches across data-generating scenarios (inner columns). Convention about power as in Fig. 2. Prediction tasks were simulated with $n = 1000$ and $p = 50$.

104 Based on the power computation, *Permfit-DNN* and *CPI-DNN* outperform the alternative methods.
 105 Thus, the use of the right learner leads to better interpretations.

106 **G Supplement Figure 3 - Computation time**

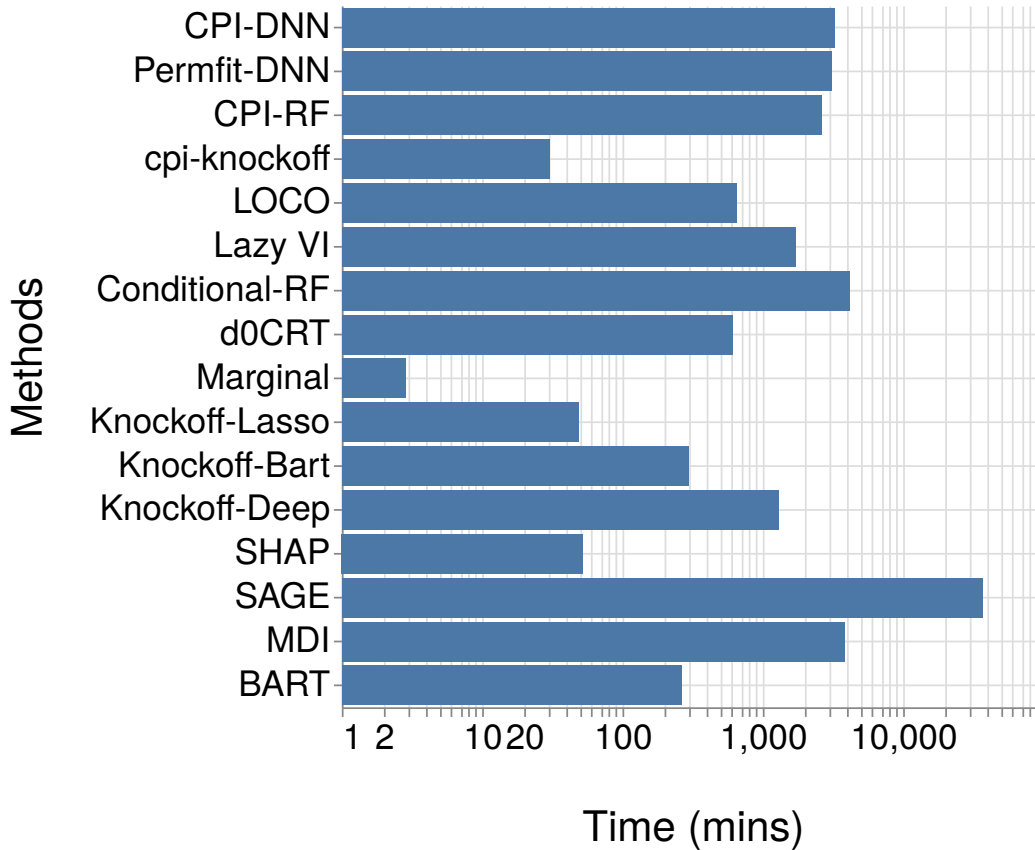


Figure 5: **Extended model comparisons:** The computation times for the different methods (with and without statistical guarantees in terms of p-values) are reported in mins with (log10 scale) per core on 100 cores. Prediction tasks were simulated with $n = 1000$ and $p = 50$.

107 The computation time of the different methods mentioned in this work (with and without statistical
 108 guarantees) is presented in Fig. 5 in mins with (log10 scale). First, we compare *CPI-RF*, *cpi-knockoff*
 109 and *LOCO* based on a Random Forest learner with $p=50$. We see that *cpi-knockoff* and *LOCO* are
 110 faster than *CPI-DNN*. A possible reason is that *CPI-DNN* uses an inner 2-fold internal validation for
 111 hyperparameter tuning (learning rate, L1 and L2 regularization) unlike the alternatives. Next, The
 112 DNN-based methods (*CPI-DNN* and *Permfit-DNN*) are competitive with the alternatives that control
 113 type-I error (*d0CRT*, *cpi-knockoff* and *LOCO*) despite the use of computationally lean learners in
 114 the latter.



Figure 6: **Evaluating predictive power:** Performance of the different base learners used in the variable importance methods (**Marginal** = {Marginal effects}, **Lasso** = {Knockoff-Lasso}, **Random Forest** = {MDI, d0CRT, CPI-RF, Conditional-RF, cpi-knockoff, LOCO}, **BART** = {Knockoff-BART, BART} and **DNN** = {Knockoff-Deep, Perffit-DNN, CPI-DNN, Lazy VI}) on simulated data with $n = 1000$ and $p = 50$ in terms of **ROC-AUC** score for the classification and **R2** score for the regression.

116 The results for computing the prediction accuracy using the underlying learners of the different
 117 methods are reported in Fig. 6. Marginal inference, performs poorly, as it is not a predictive approach.
 118 Linear models based on Lasso show a good performance in the no-interaction effect scenario. Non-
 119 linear models based on Random Forest and BART improve on the lasso-based models. Nevertheless,
 120 they fail to achieve a good performance in scenarios with interaction effects. The models equipped
 121 with a deep learner outperform the other methods.

122 **References**

- 123 Andrew P. Bradley. The use of the area under the ROC curve in the evaluation of machine learning
124 algorithms. *Pattern Recognition*, 30(7):1145–1159, July 1997. ISSN 0031-3203. doi: 10.1016/
125 S0031-3203(96)00142-2.
- 126 Przemyslaw Biecek and Tomasz Burzykowski. *Explanatory Model Analysis*. December 2020.
- 127 Emmanuel Candes, Yingying Fan, Lucas Janson, and Jinchi Lv. Panning for Gold: Model-X
128 Knockoffs for High-dimensional Controlled Variable Selection. *arXiv:1610.02351 [math, stat]*,
129 December 2017.
- 130 Hugh A. Chipman, Edward I. George, and Robert E. McCulloch. BART: Bayesian additive regression
131 trees. *The Annals of Applied Statistics*, 4(1), March 2010. ISSN 1932-6157. doi: 10.1214/
132 09-AOAS285.
- 133 Ian Covert, Scott Lundberg, and Su-In Lee. Understanding Global Feature Contributions With
134 Additive Importance Measures, October 2020.
- 135 Gilles Louppe, Louis Wehenkel, Antonio Sutera, and Pierre Geurts. Understanding variable impor-
136 tances in forests of randomized trees. page 9, January 2013.
- 137 Tuan-Binh Nguyen, Jérôme-Alexis Chevalier, Bertrand Thirion, and Sylvain Arlot. Aggregation of
138 Multiple Knockoffs. *arXiv:2002.09269 [math, stat]*, June 2020.
- 139 David S. Watson and Marvin N. Wright. Testing Conditional Independence in Supervised Learning
140 Algorithms, May 2021.
- 141 Brian D. Williamson, Peter B. Gilbert, Noah R. Simon, and Marco Carone. A general framework for
142 inference on algorithm-agnostic variable importance, September 2021.